#25-083
2025 AFS Proceedings ©American Foundry Society

The Fluidity and Solidification of Patternless Hollow Aluminosilicate Microsphere Molds vs. 3D-Printed Silica Sand

Sean Derrick, Ph.D.
Western Michigan University, Kalamazoo, Michigan, USA

ABSTRACT

It has been shown on multiple occasions that resin-bonded Hollow Aluminosilicate Microspheres (HAMs) can be subtractively machined and used as patternless molds comparable to those made from 3D-printed silica sand. However, these proofs of concepts have shown repeated anecdotal observations that the HAM material has a propensity for prolonged cooling times as well as wetting cavity details that are more difficult than that of silica-based systems. With proof of concept established, the next step is to quantitatively benchmark HAM's cooling and as-cast flow performance to verify the previous observations. To accomplish this, the following study aimed to evaluate the effects of casting fluidity and time to solidify on a known cross-section using a modified non-standard fluidity spiral. As with the previous proofs-of-concept, 3D-printed patternless silica molds were used for comparison.

Keywords: rapid casting, Industry 4.0, machinable, patternless, casting fluidity, hollow aluminosilicate microspheres, HAM, 3D-printed sand

INTRODUCTION AND BACKGROUND

Rapid Casting (RC) is a term that describes techniques and technologies that allow castings to be made faster, cleaner, and more repeatable by replacing resource-consuming conventional manual casting processes with automated aspects.[1] This process could range from integrating automatic CNC machining, robotic autonomous mold assembly, or the use of Additive Manufacturing (AM). In addition, RC is not limited to a single process, as multiple automated techniques can be combined or hybridized to increase production speed.

This author believes that RC is one of the ways to integrate Industry 4.0 into modern foundries. The end goal of which is the creation of castings that pass seamlessly from mold, melt, fill, and shakeout without the touch of human hands. Like an assembly line, each link of the casting process would be directly integrated into one another. Furthermore, this line would work flexibly and leanly, only producing what is required. Since mold making is the first link in this Industry 4.0 chain, this author also believes that automating flexible patternless molds is the key and starting point in this goal.

Presently, there are several forms of RC techniques commonly used in patternless mold-making operations, of which 3D-Printed Sand (3DP) has seen the most widespread adoption.[2-3] This is particularly the case with low-volume, prototype, and bespoke cast runs.[4] Using 3DP, digital files can yield complete molds and cores quickly without tooling or excessive lead times. However, 3DP has a fundamental deficiency that would prevent it from being directly integrated into an Industry 4.0 line. Specifically, AM processes such as 3DP require support material to create undercuts and negative draft features. This support material must be removed as part of a post-process before the mold is ready to cast. Typically, 3DP support material consists of loose unbonded sand, and once the print is complete, the desired component must be excavated from the loose media. After excavation, adhered support material, located at the transition between the desired part and the unbound supports, needs to be mechanically removed with a combination of negative and positive air as well as abrasion. Furthermore, the excavation and support removal are highly unique to parts geometry, making it difficult to automate fully.

At Western Michigan University (WMU) we have been experimenting with various patternless RC techniques that do not require post-processing and could, in theory, be directly integrated into a production line. One such technique uses a hybrid subtractive-additive approach, which has been demonstrated multiple times.[5-13] This technique has been shown to produce molds with undercuts and integral cores quickly, without the need for support material. Examples and proof of concepts of this technique have been shown in ferrous, aluminum, and copper-based alloys ranging from small test coupons to fully functional swords.[10-12] This technique has even been demonstrated with highly curvilinear parting lines, multi-section molds, and mold configurations that would not be possible in conventional non-RC techniques.[10]

To date, this technique has been demonstrated using resin-bonded Hollow Aluminosilicate Microspheres (HAM) as the mold media. During these experiments, this mold material has shown to have excellent machinable properties and, when compared to 3DP, has a smoother surface finish and sharper cavity detail. The HAMs have

also been demonstrated to be less friable and more shelf-stable than post-manufactured 3D-printed sand.[10,12] Early studies have also shown little appreciable difference in the dimensions of the components cast from HAM vs. those produced in 3DP.

During these early trials, a repetitive observation was made that HAM molds took far longer to cool and solidify than control molds from conventional silica sand systems. It was also noted that HAMs had a propensity to wet and fill thin details typically not seen in silica-based control samples. As these casting trials were proofs of concept, thus far these observations have been anecdotal and not quantitatively tracked or recorded. Now that this research is moving into a post-proof-of-concept phase it is necessary to study and track the molding and solidification behavior of the HAM material more quantitatively.

The following is an initial exploratory study into the flow, cooling, and solidification of alloys cast into HAM. For comparison, 3DP sand molds were selected because it is a currently used RC mold-making technique for direct patternless molds and was used previously in other HAM comparisons. This experiment focused on timing solidification, tracking flow distance in similar molds, and recording time to solidify in a known and controlled position and cross-section within an actual casting.

METHODOLOGY

To vet the HAM material for continued hybrid rapid casting, it is necessary to attempt a preliminary casting trial with the following objectives:

1. Determine the time to solidification of HAM at a known location and cross-section of a casting.
2. Determine the casting fluidity of HAM
3. Benchmark and compare the performance against 3D-printed sand molds.

To accomplish these objectives, the following procedure was followed:

1. Develop and prepare modified fluidity spiral molds using HAM, 3DP, and conventional pattern molding.
2. Prepare the molds with a thermocouple at a fixed cross-section within the spiral to record the casting temperature from fill to freeze.
3. Perform casting trails on the molds in a randomized pouring pattern.
4. Observe and measure the temperature at the given point within the casting.
5. Observe and measure the fluidity distance of cast samples.
6. Analysis and interpretation of results.

The molds and as-cast parts will be evaluated by:

1. Observational inspection
    a. Flash
    b. Deformation
    c. Surface defects
2. Dimensional inspection
    a. Spiral length
3. Time to solidify
    a. Thermocouple reading

DESIGN OF EXPERIMENTS

The fluidity of molten metals, specifically regarding metal casting, refers to the maximum length that liquid metal flows before it is stopped by solidification.[14] Casting Fluidity (CF) is denoted as a measure of length and should not be confused with the classical physics definition, which is a measure of viscosity. According to Lerner & Rao, “Since fluidity depends on such a large number of diverse variables, it is not theoretically feasible to determine; therefore, practical testing is recommended.” [15] Variables, such as alloy composition, head pressure, pouring temperature, velocity, and mold material composition, all play a part in CF. For this experiment, all the previously stated variables will be controlled while mold composition is varied. By controlling the variables this way, variances in the distance traveled will be represented by variances in mold material properties.

CASTING FLUIDITY

Typically, casting fluidity is evaluated by a mold containing a fixed cross-section and allowing the liquid to travel down that cross-section until freeze occurs. Mold material variations such as friction, thermal conductivity, and porosity will all play a role in affecting how quickly freeze occurs and, therefore, the length of travel. Due to the potential travel distance, fluidity experiments involve wrapping the flow channel into an Archimedean spiral to avoid excessively large mold configurations. To prevent flow restrictions, the flow channel is vented to the atmosphere with a vent at least equal to the cross-sectional area of the flow channel.

Previous publications have used two common but non-standard gravity-cast single spiral designs.[14-16] The first design uses a sprue that is distanced from the spiral so as not to present a large thermal mass to the center of the test which may retard solidification. This design also utilized a starting point positioned away from the sprue and past the gate, allowing for a more consistent measurement process. A schematic of this design is seen in Figure 1. The second spiral design, seen in Figure 2, uses a centralized sprue with fill radiating outward. This design is commonly used where space is limited and offers no gating restriction.

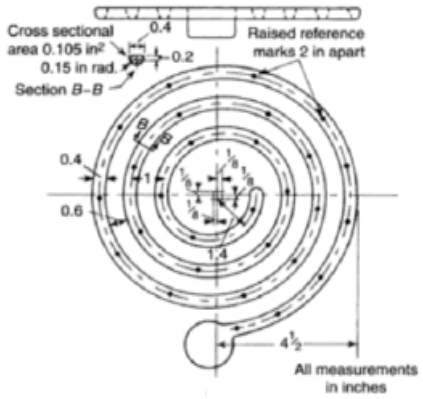

Figure 1. Offset gated Archimedean fluidity spiral schematic.[15]

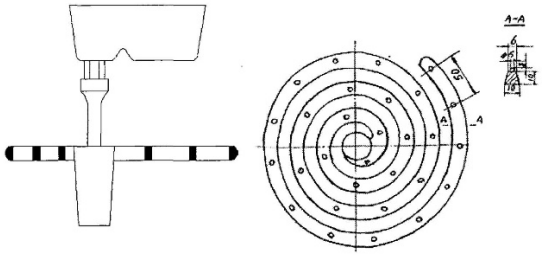

Figure 2. Center-gated Archimedean fluidity spiral schematic.[16]

In this design, a pouring basin is used to simplify Bernoulli's fluid flow equation by controlling height and velocity, Bernoulli's root equation, as seen in Equation 1 can be simplified by ignoring friction and yields in Equation 2. With a known basin wall, the head height is then controlled between the top of the basin wall and a reference point located at the well or the gate. Assuming point 1 is the reference point and point 2 is the top of the basin wall, $h_2 = 0$ as it is the reference distance. Likewise, assuming metal is poured into the basin and allowed to overflow the basin wall into the sprue $v_1 = 0$. Using these assumptions, Equation 2 can further be refined to Equation 3, and velocity is solved for in Equation 4.

Bernoulli's Equation:

$$h_1 + \frac{P_1}{\rho} + \frac{v_1^2}{2g} + F_1 = h_2 + \frac{P_2}{\rho} + \frac{v_2^2}{2g} + F_2 \qquad \textbf{Eqn. 1}$$

Ignoring Friction:

$$h_1 + \frac{v_1^2}{2g} = h_2 + \frac{v_2^2}{2g} \qquad \textbf{Eqn. 2}$$

Assuming $v_1=0$ and $h_2=0$ and simplified:

$$h_1 = \frac{v_2^2}{2g} \qquad \textbf{Eqn. 3}$$

Solving for v_2^2:

$$v = \sqrt{2gh} \qquad \textbf{Eqn. 4}$$

MODIFIED NON-STANDARD SPIRAL DESIGN

Observations from previous HAM experiments noted a highly extended cooling time compared to other mold materials. Therefore, it was assumed that additional flow length may be required. A modified, non-standard single spiral was designed specifically for this experiment using attributes from the two common designs.

Detailed in Figures 3 and 4, the design used for this experiment had an offset sprue measuring 31.75mm [1.25in] in diameter along with the second design's dedicated pouring basin that controlled head height to 76.2mm [3.00in]. Both the cope and drag were 50.8mm [2.00in.] thick with spiral detail located in the drag. The channel area of the spiral measures 76.1mm^2 [0.118in^2] with fourteen 6.35mm [0.25in] diameter measurement markings placed every 101.6mm [4in.]. Total spiral length was increased to 1.42m [56in.] from the more typical 1.2m [48in] length. To reduce fill turbulence a 4.72mm [0.186in] deep sprue well was designed into the drag. Using Equation 4 and the known head height of 76.2mm [3in], the velocity at the gate is equal to 1.22m/s [4.01 ft/s].

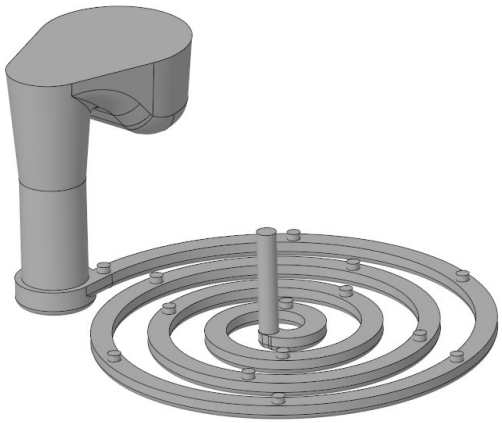

Figure 3. A 3D Model of Archimedean fluidity spiral used for this experiment.

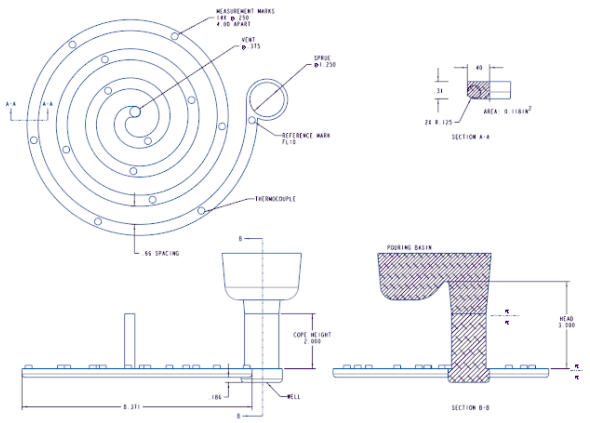

Figure 4. Full schematic of experimental fluidity spiral.

MOLD PREPARATION: HAM MATERIAL

The following section details the materials and procedures used to fabricate the fluidity spiral molds out of the designated HAM material.

Materials

The HAM material was acquired by processing down 609.6 mm dia. x 55.9 mm (24.0 in. dia. x 2.2 in.) ASK Chemical EXACTCAST™ floating cover lids. The material was prefabricated into blocks measuring 127 x 254 x 55.9 mm (5 x 10 x 2.2in.). The base HAM product consists of a proprietary HAM blend with 10% phenolic urethane by weight with HAM particle size between 40-400 µm. The following mix used for testing had the following results and properties, seen in Table 1. These properties were determined via WMU's testing lab.

Table 1. Mold Material Properties (AFS test)

	3D Printed	HAM Board
Specimen Weight (g)	24.07	7.20
Specimen Bulk Density (g/cm3)	1.58	0.52
Impact Strength (J)	0.56	0.41
Retained Strength (J)	0.25	0.33
Scratch Hardness (#)	86	89
Abrasion Loss (%)	2.43	0.73
Permeability Index (#)	193	203

Fabrication Procedure

Blocks of HAM material were harvested from cover lids and loaded into a Milltronic CNC mill. Each mold half was machined using a three-step process.

Step 1: Sizing and Roughing

Due to the size of the mold, a single block of raw material was used for each mold half. first, a raw block was surfaced milled using a 101.6 mm [4 in.] diameter fly cutter to achieve a flat, uniform, machined surface. The material was then flipped and mechanically fastened to the mill. A roughing pass using a 12.7 mm dia. x 101.6mm [0.50 in. dia x 4.0 in] two-flute carbide end mill was used for bulk material removal and to flatten the primary parting line. During this step, the sprue, well, and vents were created.

Step 2: Refinement

A medium roughing pass was then conducted using a 9.53mm Dia. X 50.8mm [0.375in. Dia. X 2.0in.] two-flute carbide endmill to refine surfaces and carve intermediate details, such as the first pass of the flow channel.

Step 3: Finishing

A finishing pass was performed using a 3.18 mm dia. x 25.4 mm [0.125in. dia. x 1.0 in] two-flue ball carbide ball end mill. The finishing pass was used for surface refinement as well as to add any radii. Swarf was actively removed during machining with positive air as well as vacuum removal. After machining the molds were cleaned using 0.07 Mpa [10 psi] compressed air. During this step, the cavity was refined, and the measurement markings were added to the cope.

Step 4: Alignment Holes.

Finally, each corner of the mold was through-drilled with a 9.53 mm diameter [0.375 in. Dia.] High-speed steel twist drill to create bolting and alignment holes for the cope and drag. Figure 5 shows an example of a HAM drag with a spiral flow channel.

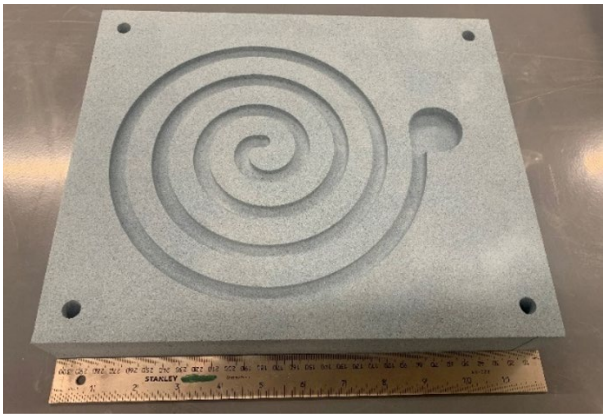

Figure 5. Machined modified non-standard fluidity spiral in HAM.

MOLD PREPARATION: 3D-PRINTED MATERIAL

For the remainder of this paper, 3DP will refer to silica sand that has been binder-jet 3D-printed using an ExOne X1 3D printing System.

Materials

This system uses AFS-GFN 80 (2 screen distribution) silica sand bonded with a furan system (1.3% BOS). The process prints the mold components in 0.3mm (0.012 in.) thick layers. Additional standardized AFS testing information is listed in Table 1.

Fabrication Procedure

The CAD data for the mold design was directly converted into STL format and sent to the 3D-Printing System. Each mold section was placed within the build volume and fabricated concurrently. The molds were oriented in the build box so that layering would occur parallel to the planned CNC machined paths of the HAM material. After fabrication, excess unbonded sand was first removed with negative pressure and then dusted using shop air. No additional post-processing occurred.

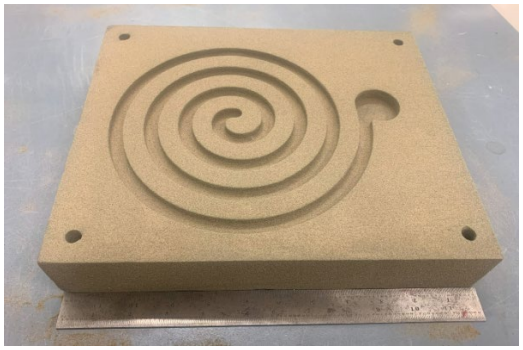

Figure 6. Machined modified non-standard fluidity spiral in 3DP.

Samples were produced and excavated from unbound material and shipped to the foundry encased in support material. Upon arrival, further excavation of loose unbound was required. First loose sand was mechanically brushed to remove bulk amounts which was followed by negative pressure suction. Finally, a 0.07 MPa [10 psi] compressed air dusting was used to clean all surfaces. Figure 6 shows a prepared 3DP drag ready for assembly.

BASINS AND CONTROL MOLDS: NO-BAKE

As there may be a difference in the performance between HAM and 3DP materials, especially concerning thermal conductivity and friction, it was determined that the pouring basin should be made from a separate material as to control and normalize any thermal or frictional loss until the metal reached the sprue. In this case, the pouring basin's resistance and conductivity to the point of $v_2 = 0$ could be held consistently between the two materials. As such, the pouring basins were constructed from conventionally molded silica sand bonded with sodium silicate no-bake binder. Although not part of the main experiment, additional molds were made entirely from the conventionally molded silica sand bonded with sodium silicate no-bake binder to further track and normalize any effect the basins may have.

Materials

In this case, a silica sand media was used with an AFS-GFN of 80 with a 2 two-screen distribution. A Chembond 4910 resin, referred to in this paper as "No-Bake," was used at 3% weight of the sand system, and # 230 catalyst was used at 10% weight of the resin.

Fabrication Procedure

First, a batch of resin-bonded silica sand was made for both the basins and spiral molds. Using prefabricated patterns, the pattern was filled and then struck off. After a sufficient setting time, each was de-molded and inspected for defects.

FINAL ASSEMBLY AND PREP

After fabrication, each of the HAM and 3DP were inspected for defects, and observations of surface finish were made. Using a 3.2 mm [.125 in.] standard twist drill an additional hole was drilled at the second spiral index location. After this the hole was cleaned with compressed air and a K-type thermocouple was inserted. The thermocouple was positioned that it would line up with the top of the mold cavity. Each thermocouple was then fixed in place, and the vent was fully sealed, using Corefix adhesive.

Carriage bolts (3/8-16) were passed through the alignment holes in the corners of each mold half and clamped with washers and nuts. The nuts were then torqued until the washer compressed into the mold and the square shank of the carriage bold was recessed into the mold media. The final mold assembly was inspected for gaps between parting lines. The molds were glued around the entirety of the cavity perimeter using the adhesive. The copes and drags were then assembled, aligned, and allowed to cure with an 11.3 Kg [25 lb.] compressive load.

Each basin was attached to its respective mold with adhesive. A continuous bead was made around the sprue and a secondary continuous bead made around the perimeter of the basin. The basins were aligned via the sprue interface and allowed to cure. An example of the finished molds, including thermocouples and basins, is shown in Figure 7.

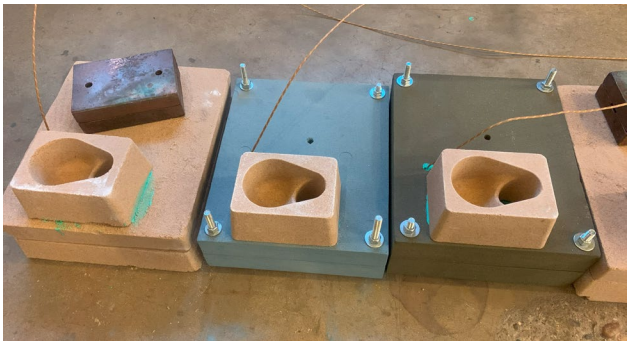

Figure 7. Assembled experimental molds shown with basins and thermocouples.

MELT AND POURING

The molds were manually poured in A319 aluminum (15s fill, temperature at pouring ladle 1350F (732.2C)). A random number generator randomly selected the three

mold types for the pouring order, which is found in Table 2, located in the analysis section.

RESULTS AND OBSERVATIONS

The following section will discuss both the visual and quantitative results found before, during, and after the fluidity casting trial. Particular attention is paid to the direct comparison of HAM vs. 3DP.

MOLD OBSERVATIONS

Before casting, the molds were visually inspected with particular emphasis on the mold cavity. Both molds rendered cavities with comparable geometries, as seen in Figure 8. No obvious voids, defects, or inconsistencies were noted between the materials. The HAM had a much smoother surface appearance, whereas 3DP appeared rough. The 3DP material appeared to be more friable even after the final clean-off and prep.

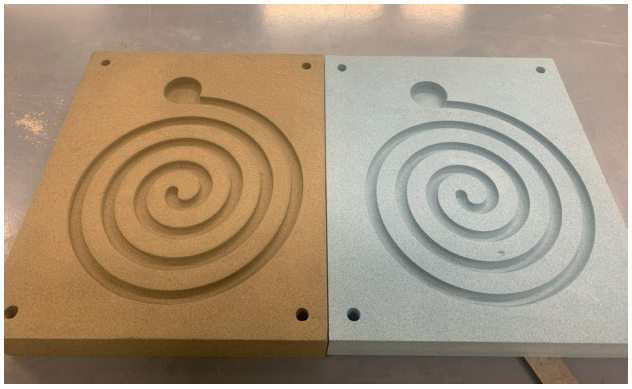

Figure 8. Patternless drag comparison between 3DP (left) and HAM (right).

Under closer inspection (Figure 9) the cavity details appeared sharper and less rounded in the HAM material compared to the 3DP. This was particularly noticeable around the parting line, where the edges were rounded. Additionally, the curvature of the 3DP showed distinctive layer lines, whereas the HAM was smoother.

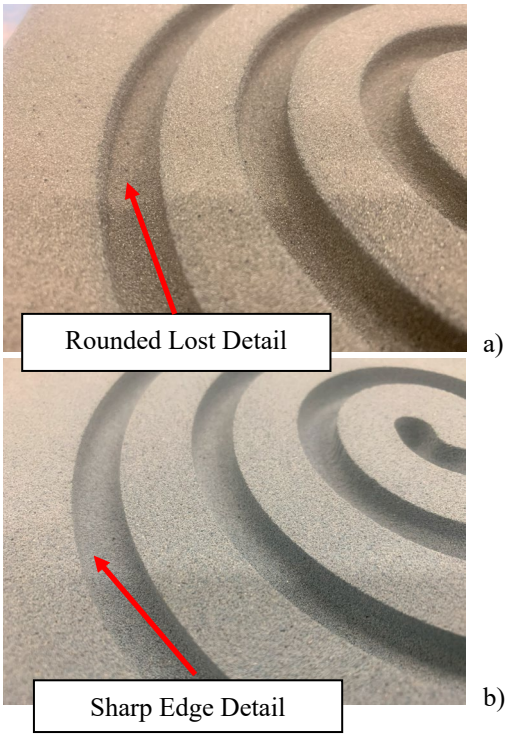

Figure 9. Mold detail comparison between 3DP (a) and HAM (b).

CASTING OBSERVATIONS

All molds were filled until either a leak was detected, the sprue would no longer accept additional liquid, or the end vent showed signs of overflow. During the pour, the first mold, which was made from No-Bake, suffered a miss-run when a leak formed at the parting line. The remaining molds plus all HAM and 3DP filled without issue. The first two HAM molds filled to the point where liquid visibly came from the vent at the end of fill, shown in Figure 10. None of the 3DP or No-Bake samples experienced this excessive fill.

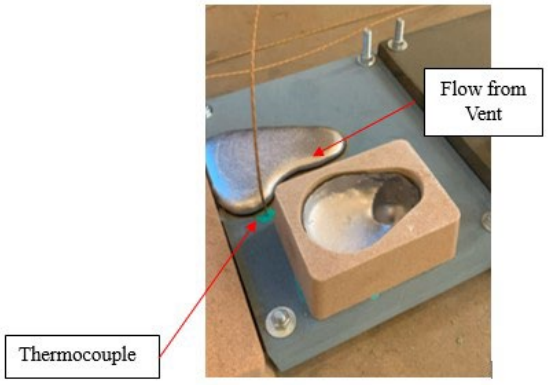

Figure 10. The HAM mold after pour showing flow emerging from end of fill vent.

No visible smoke, gas, or sound emanated from the No-Bake samples. Discoloration, not directly contacted by aluminum, was noted in the No-Bake basins only. The HAM samples emanated a clear gaseous material for a prolonged period. No discoloration or sound was noted on the cope or parting line when not in direct contact with poured aluminum, i.e., overflow. Large amounts of black smoke along with audible cracking and popping sounds came from 3DP and all copes showed discoloration.

SHAKEOUT

The HAM specimens had a longer cooling time visually than the other two materials. The sprues were mechanically tapped to determine solidification. For safety, the molds were left to cool for sixty minutes before shakeout. The HAM and 3DP molds were shaken out by first removing the carriage bolts and then separating at the part line. The glued samples had to be mechanically pried apart at the parting line.

In all samples, the cast sample remained with the cope upon separation. HAM and No-Bake had a great amount of material adhered between the coils of the spiral while 3DP separated cleanly in all instances. The HAM material showed a greater amount of discoloration, followed by the 3DP samples.

CASTING RESULTS

The 3DP samples filled cleanly with little flash. The casting appeared clean and metallic with a yellow discoloration noticed in the three measurement markings. None of the specimens reached the end of the fill. The measurement markings of each specimen began to round over halfway during the fill length. The results can be seen in Figure 11.

Figure 11. As-cast spirals in 3DP from last poured (left) to first poured (right).

In contrast, the HAM samples all reached the vent and thus the maximum allowable measurement as seen in Figure 12. The first two samples that were poured experienced significant vent flow. Each sample had a significant dark discoloration and granular media attached loosely to the surface. The first two specimens had their sprues fall to the top level of the cope i.e., 50.8 mm [2.0 in.] from the parting line as flow equalized with the vent height. The last specimen poured began to fill the vent and kept its pouring basin. All measurement locations were fully formed without rounding or visual signs of premature solidification.

Figure 12. As-cast spirals in HAM from last poured (left) to first poured (right).

Figure 13. As-cast spirals in No-Bake from last poured (left) to first poured (right).

Finally, only two of the No-Bake specimens were filled without leaking, as seen in Figure 13. However, heavy flash was evident in all samples. There was no visible discoloration of the cast surface with isolated areas of retained mold attached to the cast surface. There was a noticeable drop in fluidity length between the two surviving samples, with the longest being the second sample poured. Significant rounding of the measurement markers was noticed in both samples with elongated narrowing of the flow bath one to two markings away from end-of-fill.

TEMPERATURE RESULTS

The recorded temperatures from the final 3DP and HAM samples were nonviable, leaving only two readings per experiment group. The readings are shown in Figure 14.

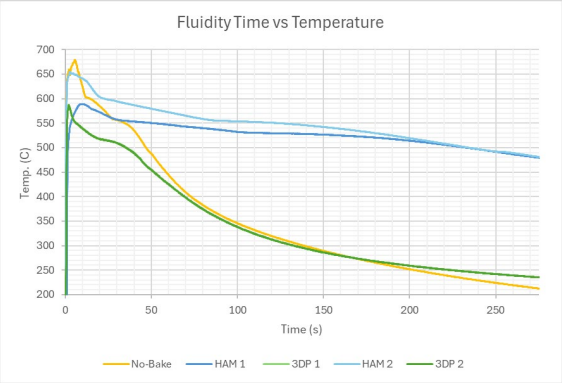

Figure 14. Thermocouple data shown as time vs. temperature.

DATA ANALYSIS AND DISCUSSION

As charted in Table 2, the HAM samples had distinctively longer spiral lengths. All samples traveled the maximum distance, or greater, with an average recorded length of 1422.4 mm [56 in.]. Furthermore, the first two HAM specimens easily filled the vent, indicating a greater flow was possible. The third specimen reached the precise start of the vent and showed no signs of premature freeze. The 3DP specimens had a lower spiral length with an average of 1099.8 mm [43.3 in.] across the three samples. The No-Bake specimens experienced the shortest spiral length, averaging 718 mm [28.3 in.] however, flash and parting line leaks were evident in all three. As expected, each sample traveled progressively less relative to the pouring order, indicating that the melt cooled as the pour order progressed.

Table 2. Experiment Fluidity Results & Pouring Order

	Pouring Order								
	1	2	3	4	5	6	7	8	9
Material	No-Bake	HAM	3DP	No-Bake	HAM	3DP	No-Bake	3DP	HA
Thermocouple	Yes	Yes	Yes	No	Yes	Yes	No	Yes	Ye
Fluidity [in.]	N/A	56+	46	35.5	56+	45	21	39	56

Upon review of the thermocouple data, several observations are apparent. First and foremost, the HAM samples had a slower cooling rate and prolonged time to reach solidus. The 3DP reached solidus in an average of 22.4 seconds after initial wetting while the No-Bake sample reached solidus in 44.0 seconds. This is in stark contrast to the HAM samples which took an average of 200.3 seconds to reach 516C (961F) after initial wetting. This indicates a substantial reduction in time to solidify. Likewise, the HAM specimens remained above 400C (752F)for the duration of the recorded time, while both No-Bake and 3DP had cooled to below 300C (572F), indicating a prolonged reduction in cooling.

Isolating the collected data and focusing on behavior during liquidus temperatures, found in Figure 15, shows an interesting reading for the second HAM sample. The second No-Bake sample was not equipped with a thermocouple and is missing from this chart. This makes the second HAM specimen the fifth specimen poured. Despite this, the fifth specimen showed a pronounced spike in maximum recorded temperature. It should be noted that the melt was not reheated in any way once the first specimen was poured. However, despite this spike, the cooling rate of both HAM samples is distinctively longer than 3DP or No-Bake.

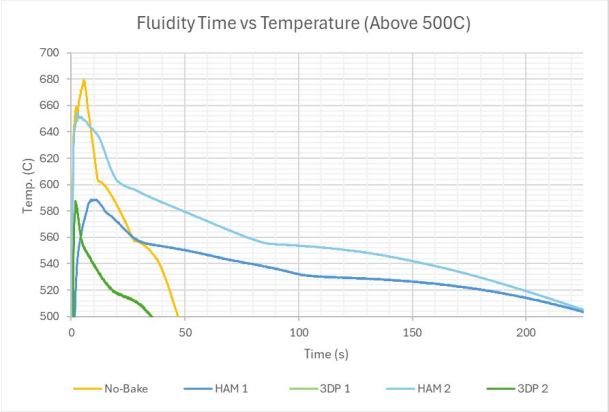

Figure 15. Thermocouple data shown as time vs. temperature (data collected above 500C/932F).

When the cooling behavior of HAM and 3DP are extrapolated over the time taken to reach 450C (842F), as shown in Figure 16, both mold materials show similar overall cooling behavior. This further indicates that the mold material behaves uniformly throughout the cooling process. However, this comparison further indicates that there may be potential metallurgical differences between the two materials. The alloy remains in thermal regions, which may allow for differing intermetallic and phase development within the aluminum alloy.

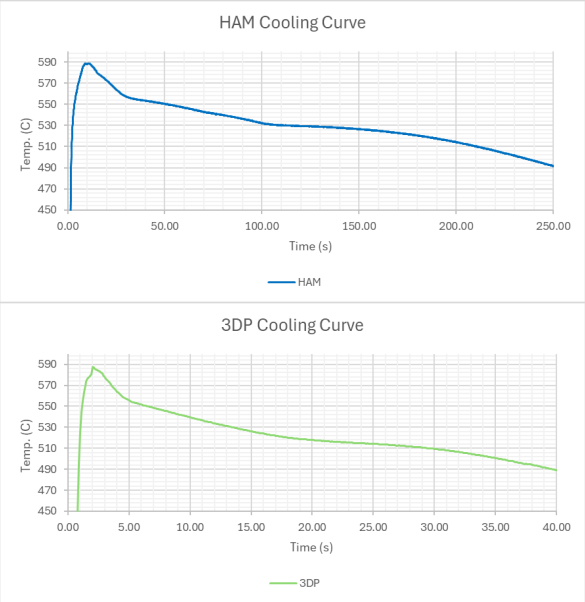

Figure 16. Thermocouple data shown as time vs. temperature shown from initial pour until 400C (752F). HAM (Top) and 3DP (Bottom).

CONCLUSIONS

This data corroborates the anecdotal observations of HAM molds being noticeably longer to cool and solidify than silica-based molds. The dramatic difference in both fluidity length and time to solidify indicates that HAM is substantially more insulative than conventional silica-based systems. Unfortunately, due to the limited dataset and the HAM specimens reaching maximum experimental length, it is not possible to establish a definitive statistical significance with this single experiment. However, the results are plain: the HAM material allowed for fluidity travel to a minimum of 33% more than the 3DP samples in these instances. Likewise, this is further corroborated as HAM's time to reach solidus, with a controlled cross-section after initially wetting, is 9 times longer than that of the 3DP samples.

RECOMMENDATIONS

It is recommended that a follow-up study be pursued to establish the statistical significance of both the fluidity distance and the time to solidify. It is also recommended that follow-up studies be conducted to determine the metallurgical effects of the prolonged cooling that HAM has on cast alloy. Due to the lengthened time at elevated temperatures, it is theorized that the microstructures and cast porosity may vary between the castings. Finally, due to the increased fluidity and reduced cooling, it is advised that an exploratory study be conducted to determine what level of detail can HAM be wet vs that of silica-based systems. Due to the ease of machining and increased fluidity there may be applications in using HAM strategically as inserts or as full molds to increase the level of cast detail in production molds.

ACKNOWLEDGEMENTS

Special thanks to Dr. Robert Tuttle and Dr. Sam Ramrattan of WMU for their help and critique in running this experiment. A big thank you to Joseph Hutto of Howell Foundry for facilitating the 3DP samples used for this experiment. Without your support, this experiment would not have happened.

REFERENCES

1. Tromans, G., "Developments in Rapid Casting," *Scitech Book News* 03 2004ProQuest. Web. 20 Sep. 2014.
2. Chhabra, M., Singh, R., "Rapid Casting Solutions: A Review," *Rapid Prototyping Journal*, Vol. 17 Iss: 5, pp. 328-350.
3. Gill, S. S., & Kaplas, M., "Comparative Study of 3D Printing Technologies for Rapid Casting of Aluminum Alloy," *Materials and Manufacturing Processes*, 24(12),1405-1411 (2009). doi:10.1080/10426910902997571
4. Upadhyay, M., Sivarupan, T., & Mansori, M. E. (2017), "3D printing for rapid sand casting—A review," *Journal of Manufacturing Processes*, 29, 211-220. doi:10.1016/j.jmapro.2017.07.017
5. Bohra, H., Ramrattan, S., Joyce, M., "Evaluation of a 3D Light Cured Sand for Rapid Casting Technology," *AFS Transactions*, 14-062.
6. Kerschbaumer, M., Ernst, G., " Hybrid Manufacturing Process for Rapid High-Performance Tooling combining High-Speed Milling and Laser Cladding," *23rd International Congress on Applications of Lasers and Electro-Optics* (2004).
7. Rebros, M., Ramrattan, S., Joyce, M., Ikonomov, P., "Behavior of 3D printed Sand at Elevated Temperature," *111th AFS Metalcasting Congress*, *AFS Transactions*, Houston, TX (15-18 May 2007).
8. Ikonomov, P., Ramrattan S., Konkel, M., "Hybrid System for Producing Functional Casting Prototypes," *AFS Transactions*, 20-075.
9. Derrick, S., Ramrattan, S., Konkel, M., "An Investigation into processing parameters for 3D-Light Cured Sand used in Rapid Casting," *119th AFS Metalcasting Congress* (21-23 April 2015).
10. Derrick, S., Ramrattan, S., "Rapid Casting using Machinable Molds Compared to 3D-Printing Technology," Metal *126th AFS Metalcasting Congress* (23-26 April 2022).
11. Derrick, S., Ramrattan, S., "Casting a High-Performance 440C Celtic Leaf Sword Using

Machinable Rapid Molds" *127th AFS Metalcasting Congress* (25-27 April 2023).
12. Derrick, S., Ramrattan, S., "Evaluating the Dimensional Accuracy of a Machinable Mold Media Using 3D-Printed Patternless Silca for Comparison," *127th AFS Metalcasting Congress* (25-27 April 2023)
13. Ramrattan, S., Wells, L., Patel, P., & Shoemaker, J., "Qualification of chemically bonded sand systems using a casting trial for quantifying interfacial defects," *International Journal of Metalcasting*, 12(2), 214–223 (2017). https://doi.org/10.1007/s40962-017-0166-3 (Link last accessed 03-26-25.)
14. Flemings, M.C., "Solidification Processing," New York: McGraw-Hill (1974).
15. Lerner, Y.S., & Rao, P.N., "Metalcasting: Principles & Techniques," American Foundry Society (2013).
16. DiSabatino, M., et al. "An Improved method for fluidity measurement by gravity casting of spirals in sand moulds," *2005 International Journal of Cast Metals Research,* Vol. 18, No. 1 (2005).